

## Spray-Mediated Enthalpy Flux to the Atmosphere and Salt Flux to the Ocean in High Winds

EDGAR L ANDREAS

*NorthWest Research Associates, Inc., Lebanon, New Hampshire*

(Manuscript received 2 February 2009, in final form 14 October 2009)

### ABSTRACT

Forecasts for the intensity and intensity changes of tropical cyclones have not improved as much as track forecasts. In high winds, two routes exist by which air and sea exchange heat and momentum: by spray-mediated processes and by interfacial transfer right at the air–sea interface, the only exchange route currently parameterized in most storm models. This manuscript quantifies two processes mediated by sea spray that could affect predictions of storm intensity when included in coupled ocean–atmosphere models. Because newly formed spray droplets cool rapidly to an equilibrium temperature that is lower than the air temperature, they cool the ocean when they reenter it, clearly transferring enthalpy from sea to air. These reentrant droplets proliferate in storm winds and are predicted to transfer enthalpy at a rate comparable to interfacial processes when the near-surface wind speed reaches  $30 \text{ m s}^{-1}$ . Because reentrant spray droplets give up pure water to the atmosphere during their brief lifetime, they return to the sea saltier than the surface ocean water and thus also constitute an effective salt flux to the ocean (also related to a freshwater flux and a buoyancy flux). That is, reentrant spray droplets add enthalpy to the atmosphere to power storms and destabilize the ocean by increasing the salinity at the surface. Both processes can affect storm intensity. This manuscript demonstrates the magnitudes of the spray enthalpy and salt fluxes by combining a sophisticated microphysical model and data from the study of Humidity Exchange over the Sea (HEXOS) and the Fronts and Atlantic Storm-Tracks Experiment (FASTEX). It goes on to develop a fast algorithm for predicting these two fluxes in large-scale models.

### 1. Introduction

Evaporating sea spray droplets release water vapor to the near-surface atmosphere. Spray droplets also lose sensible heat to the atmosphere because they originate with the same temperature as the surface ocean but cool rapidly to a temperature lower than the ambient air temperature (Andreas 1990, 1995). Because the sensible heat exchange occurs three orders of magnitude faster than the vapor exchange, spray droplets extract sensible heat from the atmosphere to evaporate and, thus, reclaim some of the sensible heat they have lost. Quantifying the net heating of the atmosphere that is mediated by spray has therefore been illusive.

The rate of this net heating is usually termed the enthalpy flux and is the sum of the total air–sea sensible and latent heat fluxes (Businger 1982). I use the adjec-

tive “total” here to recognize the possibility that the relevant fluxes comprise contributions from both the usual *interfacial* sensible and latent heat fluxes (molecular transfer directly across the air–sea interface) and the *spray-mediated* fluxes.

Emanuel (1995) explained that, for studying the intensity of tropical cyclones, the enthalpy flux—rather than the individual fluxes of sensible and latent heat—is the “energetically important transfer” from sea to air. He therefore had trouble envisioning how spray could affect storm intensity; that is, throwing a blob of seawater into the air and letting it cool and evaporate there did not seem to transfer any enthalpy from sea to air.

Andreas and Emanuel (2001), however, solved this thermodynamics puzzle. If some of the cooled spray droplets fall back into the sea, they obviously cool the ocean and complete the cycle of enthalpy exchange between sea and air. Andreas and Emanuel termed these *reentrant* spray droplets and invoked them to demonstrate that sea spray can transfer enthalpy across the air–sea interface. Moreover, Andreas and Emanuel derived a simple parameterization for the enthalpy flux carried by

---

*Corresponding author address:* Dr. Edgar L. Andreas, NorthWest Research Associates, Inc. (Seattle Division), 25 Eagle Ridge, Lebanon, NH 03766-1900.  
E-mail: eandreas@nwra.com

these reentrant droplets by using Andreas and DeCosmo's (1999, 2002) analysis of the turbulent heat flux data from the Humidity Exchange over the Sea (HEXOS) experiment.

Here, I update Andreas and Emanuel's (2001) parameterization for the spray enthalpy flux by supplementing the HEXOS data with a larger set of turbulent heat flux data from the Fronts and Atlantic Storm-Tracks Experiment (FASTEX; Joly et al. 1997; Persson et al. 2005). Because this parameterization is theoretically based and tuned with data for wind speeds up to  $20 \text{ m s}^{-1}$ , I have some confidence that it can be extrapolated up to the lower limits of hurricane-strength winds—say to  $40 \text{ m s}^{-1}$ .

As spray droplets evaporate, they become increasingly saline. By logically following the concept of reentrant spray droplets mentioned above, we see that these droplets must also constitute an effective salt flux to the ocean when they fall back into the sea. To my knowledge, no one has estimated this spray salt flux before or even anticipated it. From the HEXOS and FASTEX data and our previous analysis of the spray fluxes that they imply (Andreas et al. 2008), I here make the first estimate of the spray salt flux to the ocean. Realize, also, what I term the salt flux is directly related to quantities variously termed the freshwater flux or the buoyancy flux.

Even in winds as low as  $15\text{--}20 \text{ m s}^{-1}$ , the spray salt flux can be 10% of the salt flux resulting from interfacial evaporation. I therefore also develop a fast algorithm for estimating the spray-mediated salt flux to the ocean. In hurricane-strength winds, this spray salt flux should have a significant influence on ocean mixing.

## 2. Reentrant spray

Andreas and DeCosmo (2002) and Andreas et al. (2008) modeled the total air–sea latent ( $H_{L,T}$ ) and sensible ( $H_{s,T}$ ) heat fluxes as linear combinations of interfacial and spray contributions:

$$H_{L,T} = H_L + \alpha \bar{Q}_L \quad \text{and} \quad (2.1a)$$

$$H_{s,T} = H_s + \beta \bar{Q}_s + (\gamma - \alpha) \bar{Q}_L. \quad (2.1b)$$

Here,  $H_L$  and  $H_s$  are interfacial latent and sensible heat fluxes estimated with the Coupled Ocean–Atmosphere Response Experiment (COARE) version 2.6 bulk flux algorithm (Fairall et al. 1996). Molecular processes at the air–sea interface control these interfacial fluxes (e.g., Liu et al. 1979). The  $\bar{Q}_L$  and  $\bar{Q}_s$  are “nominal” spray fluxes of latent and sensible heat. These come from Andreas's (1989, 1990, 1992) full microphysical spray model and reflect flux contributions integrated over all spray droplets with initial radii,  $r_0$ , between 1.6 and  $500 \mu\text{m}$ .

I call  $\bar{Q}_L$  and  $\bar{Q}_s$  nominal fluxes because they have proper theoretical dependence on wind speed, humidity, and air and sea surface temperatures but are still somewhat uncertain—mainly because of uncertainties in the spray generation function. The  $\alpha$ ,  $\beta$ , and  $\gamma$  are small, nonnegative coefficients that allowed us to tune this model with the HEXOS and FASTEX data. In (2.1),  $\alpha \bar{Q}_L$  is the spray latent heat flux, and  $\beta \bar{Q}_s$  is the direct spray sensible heat flux. The  $\gamma \bar{Q}_L$  term is a small feedback effect that may be necessary because the evaporating spray cools the near-surface air, thereby increasing the air–sea temperature difference and enhancing  $H_s$  above what the COARE algorithm would predict. This term, thus, is an indirect spray effect on the sensible heat flux.

For their analysis, Andreas et al. (2008) interpreted  $H_{L,T}$  and  $H_{s,T}$  as the HEXOS and FASTEX fluxes obtained by eddy-covariance measurements at heights of 8–20 m above the sea surface. In modeling applications, once (2.1) is tuned with data, their predictions of  $H_{L,T}$  and  $H_{s,T}$  could serve as the lower flux boundary conditions for an atmospheric model or the upper-boundary conditions for an ocean model.

The total enthalpy flux is the sum of (2.1a) and (2.1b):

$$Q_{\text{en},T} = H_{L,T} + H_{s,T} = H_L + H_s + \beta \bar{Q}_s + \gamma \bar{Q}_L. \quad (2.2)$$

Notice here, the main spray latent heat flux term,  $\alpha \bar{Q}_L$ , drops out with this summation, as it should. The only effect of spray latent heat on the total enthalpy flux is thus through the  $\gamma \bar{Q}_L$  term, the presumably small feedback term. Meanwhile, the sensible heat flux associated with reentrant spray, the  $\beta \bar{Q}_s$  term, is the primary mechanism by which spray affects enthalpy transfer.

Figures 1 and 2 show my conceptual picture of how spray droplets affect the air–sea fluxes of enthalpy and salt.

Figure 1 depicts spray droplets forming with initial temperature  $T_s$ , the sea surface temperature. All droplets cool within seconds, however, to an equilibrium temperature  $T_{\text{eq}}$  that is lower than the air temperature (and usually lower than the sea surface temperature) and depends on environmental conditions and the droplet radius at formation,  $r_0$  (Andreas 1990, 1995, 1996). The droplets also lose water by evaporation (not depicted in Fig. 1). Because this is a slower process than the temperature evolution and therefore occurs while the droplets are at  $T_{\text{eq}}$ , the latent heat for that evaporation must reflect a conversion from sensible heat in the near-surface air [i.e., the  $\alpha \bar{Q}_L$  terms in (2.1b)]. As a result, whether spray droplets ultimately heat or cool the air is not obvious at first.

In fact, if droplets were to evaporate entirely (as freshwater droplets could) or were to stay suspended indefinitely, their net effect would be hard to deduce. But the

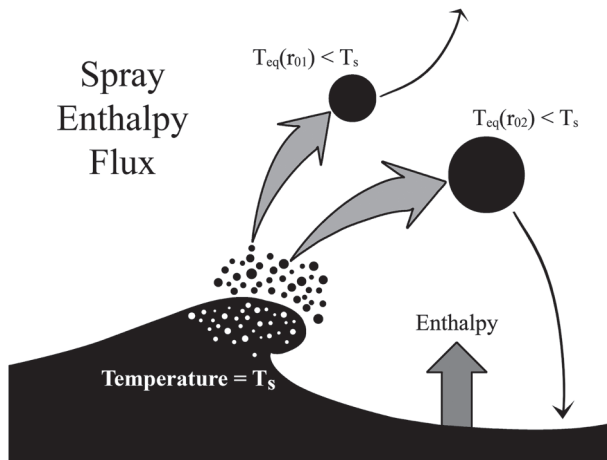


FIG. 1. How sea spray droplets contribute to the flux of enthalpy from sea to air. All droplets cool rapidly from their initial temperature  $T_s$  to an equilibrium temperature  $T_{eq}$  that depends on environmental conditions and initial droplet radius (denoted  $r_{01}$  and  $r_{02}$ ;  $r_{01} < r_{02}$ ). Smaller droplets remain suspended and do not have an obvious effect on the enthalpy flux, but larger droplets fall back into the sea and clearly cool the ocean, demonstrating that the spray is responsible for a net flux of enthalpy.

larger droplets fall back into the sea. Because  $T_{eq} < T_s$ , these clearly cool the ocean. This thought experiment therefore demonstrates that sea spray transfers enthalpy from sea to air.

Andreas (1990, 1992) introduced three droplet time scales to help us decide what “large” droplets are. I have been using as an estimate of a droplet’s residence time  $\tau_f$  the ratio of one-half the significant wave height ( $H_{1/3}$ ) to the droplet’s terminal fall speed ( $u_f$ ):

$$\tau_f = \frac{H_{1/3}}{2u_f}. \quad (2.3)$$

The temperature evolution time  $\tau_T$  is the  $e$ -folding time for the droplet’s cooling:

$$\frac{T(t) - T_{eq}}{T_s - T_{eq}} = \exp\left(\frac{-t}{\tau_T}\right), \quad (2.4)$$

where  $T$  is the droplet’s instantaneous temperature and  $t$  is the time since formation. The radius evolution time  $\tau_r$  is the corresponding  $e$ -folding time for the droplet’s evaporation to an equilibrium radius,  $r_{eq}$ :

$$\frac{r(t) - r_{eq}}{r_0 - r_{eq}} = \exp\left(\frac{-t}{\tau_r}\right), \quad (2.5)$$

where  $r$  is the droplet’s instantaneous radius.

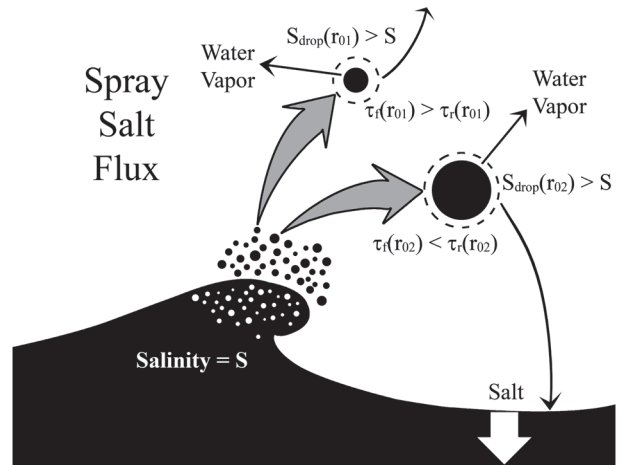


FIG. 2. How sea spray droplets produce a flux of salt to the ocean. All droplets start with ocean salinity  $S$  but become more saline through evaporation. Droplets with smaller initial radii ( $r_{01}$ ) lose water vapor more quickly than larger droplets (radius  $r_{02}$ ), but the smaller droplets can remain suspended indefinitely. The larger reentrant droplets, on the other hand, deliver excess salt to the ocean surface. I judge as large droplets those for which their residence time ( $\tau_f$ ) is less than their radius evolution time ( $\tau_r$ ).

Andreas (1992), Andreas and DeCosmo (1999), and Andreas et al. (1995) show plots that compare  $\tau_r$ ,  $\tau_T$ , and  $\tau_f$ . All of these time scales depend on initial droplet radius, air temperature and humidity, and surface salinity. The time  $\tau_f$  also depends on the wind speed and water depth because I use Andreas and Wang’s (2007) formulation to estimate  $H_{1/3}$  in the absence of measurements of  $H_{1/3}$ . For all droplets,  $\tau_T \ll \tau_r$ .

When the discussion is about enthalpy transfer, large droplets are those that fall back into the sea locally; they have  $\tau_f$  values of, say, 10 s or less. Droplets with  $r_0$  greater than 20–120  $\mu\text{m}$ , depending on wind speed, are therefore large droplets within this context (e.g., Andreas and DeCosmo 1999).

Figure 2 sketches how spray droplets produce an effective salt flux to the ocean. Here, droplets start with the same salinity,  $S$ , as the ocean surface. Because of evaporation, though, droplet salinity increases from  $S$ . Smaller droplets, which evaporate more quickly, become saltier than large droplets. But many of these smaller droplets remain suspended indefinitely; only the larger reentrant spray droplets deliver excess salt to the ocean. Equivalently, the water lost by these reentrant droplets constitutes a freshwater loss from the ocean. Later, I will assume that large droplets in this context are ones for which  $\tau_f < \tau_r$ . That is, their atmospheric residence time is less than their radius evolution time scale. Depending on wind speed,  $r_0$  is greater than 20–50  $\mu\text{m}$  for droplets that contribute to the salt flux [see Andreas and DeCosmo’s (1999) plot of  $\tau_f$  and  $\tau_r$ ].

### 3. Data

Andreas et al. (2008) described the HEXOS and FASTEX datasets. Briefly, the HEXOS data came directly from tabulations in DeCosmo's (1991) thesis. Andreas and DeCosmo (2002) described some preprocessing that we did to obtain the required variables. The HEXOS set includes eddy-covariance measurements of the friction velocity ( $u_*$ ) and the total sensible ( $H_{s,T}$ ) and latent ( $H_{L,T}$ ) heat fluxes on the Meetpost Noordwijk platform in the North Sea. Smith et al. (1992), Katsaros et al. (1994), and DeCosmo et al. (1996) provided thorough descriptions of the instruments and the measurements. The HEXOS set contains 175 runs with turbulent fluxes and associated mean meteorological quantities collected in 10-m winds up to  $18.3 \text{ m s}^{-1}$ .

The FASTEX set also includes eddy-covariance measurements of the three turbulent fluxes ( $u_*$ ,  $H_{s,T}$ , and  $H_{L,T}$ ) and associated mean meteorological quantities. These came from instruments placed on the bow mast of the R/V *Knorr* while the ship made a winter transect across the North Atlantic from England to Nova Scotia (Persson et al. 2005). The FASTEX set includes 322 hourly flux measurements in winds up to  $22 \text{ m s}^{-1}$ .

Both the HEXOS and FASTEX sets also include measurements of the significant wave height,  $H_{1/3}$ , for use in (2.3). Andreas et al. (2008) explain other details of how we manipulated the HEXOS and FASTEX data to compute the values of  $H_s$ ,  $H_L$ ,  $\overline{Q}_S$ , and  $\overline{Q}_L$  in (2.1) and (2.2).

### 4. Spray-mediated enthalpy flux

The analysis by Andreas et al. (2008) yielded the values for  $H_s$ ,  $H_L$ ,  $\overline{Q}_S$ , and  $\overline{Q}_L$  that I use here. I estimate  $H_s$  and  $H_L$  from the COARE version 2.6 bulk flux algorithm (Fairall et al. 1996), with some slight changes as described by Andreas et al. Fairall et al. (2003) updated the COARE algorithm to version 3.0. I prefer version 2.6 for my application here, however, because its calculations of temperature ( $z_T$ ) and humidity ( $z_Q$ ) roughness lengths, which are required for computing  $H_s$  and  $H_L$ , are based on the surface renewal theory of Liu et al. (1979). Because this algorithm is theoretically based and proven accurate for treating the interfacial sensible and latent heat fluxes in winds up to  $10 \text{ m s}^{-1}$  (e.g., Fairall et al. 1996; Grant and Hignett 1998; Chang and Grossman 1999), it should still be accurate when extrapolated to higher wind speeds.

In the COARE version 3.0 algorithm, on the other hand, Fairall et al. (2003) determined  $z_T$  and  $z_Q$  by fitting data collected in winds up to  $20 \text{ m s}^{-1}$ . My previous work has demonstrated that spray contributions to the heat

fluxes become significant when winds reach  $10\text{--}15 \text{ m s}^{-1}$ . Hence, I believe that this newer COARE algorithm mixes spray and interfacial fluxes in its estimates of  $z_T$  and  $z_Q$  and, therefore, is not useful for separating spray and interfacial contributions in the HEXOS and FASTEX datasets.

Andreas et al. (2008) computed  $\overline{Q}_S$  and  $\overline{Q}_L$  from Andreas's (1989, 1990, 1992) microphysical spray model. The relevant equations for  $\overline{Q}_S$  are

$$Q_S(r_0) = \rho_w c_w (T_s - T_{\text{eq}}) \left[ 1 - \exp\left(\frac{-\tau_f}{\tau_T}\right) \right] \left( \frac{4\pi r_0^3}{3} \frac{dF}{dr_0} \right) \quad (4.1)$$

and

$$\overline{Q}_S = \int_{r_1}^{r_2} Q_S(r_0) dr_0. \quad (4.2)$$

In (4.1),  $\rho_w$  ( $1000 \text{ kg m}^{-3}$ ) is the density of seawater, and  $c_w$  ( $4000 \text{ J kg}^{-3}$ ) is the specific heat of seawater (e.g., Andreas 2005b). In (4.2),  $r_1$  and  $r_2$  are the smallest and largest droplets that contribute significantly to the integral.

The spray generation function,  $dF/dr_0$ , is a key component of (4.1). It predicts the rate at which droplets of radius  $r_0$  are produced at the sea surface. Consequently,  $(4\pi r_0^3/3) dF/dr_0$  is the total volume production rate for all droplets of radius  $r_0$ . Andreas et al. (2008) used the Fairall et al. (1994) form for this function [equations in Andreas (2002)]. For this function  $r_1 = 1.6 \text{ }\mu\text{m}$  and  $r_2 = 500 \text{ }\mu\text{m}$ .

I interpret (4.1) as the contribution to the spray sensible heat flux from each droplet size  $r_0$ . Equation (4.2) therefore gives the total (nominal) spray contribution since it represents an integral over all droplets.

The equations for the spray latent heat flux are (Andreas et al. 2008)

$$Q_L(r_0) = \rho_w L_v \left\{ 1 - \left[ \frac{r(\tau_f)}{r_0} \right]^3 \right\} \left( \frac{4\pi r_0^3}{3} \frac{dF}{dr_0} \right) \quad \text{for} \quad \tau_f \leq \tau_r, \quad (4.3a)$$

$$Q_L(r_0) = \rho_w L_v \left[ 1 - \left( \frac{r_{\text{eq}}}{r_0} \right)^3 \right] \left( \frac{4\pi r_0^3}{3} \frac{dF}{dr_0} \right) \quad \text{for} \quad \tau_f > \tau_r, \quad (4.3b)$$

and

$$\overline{Q}_L = \int_{1.6}^{500} Q_L(r_0) dr_0. \quad (4.4)$$

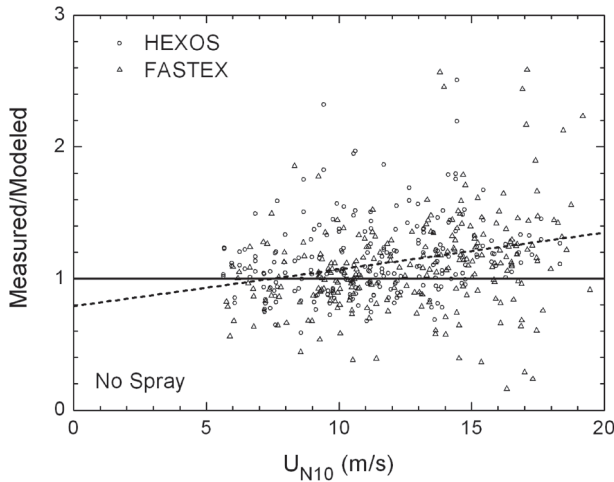


FIG. 3. The ratio of HEXOS and FASTEX measurements of the total enthalpy flux ( $Q_{en,T} = H_{L,T} + H_{s,T}$ ) to the enthalpy flux modeled as just the interfacial contribution (i.e., no spray effect;  $Q_{en,int} = H_L + H_s$ ). The abscissa is the neutral-stability wind speed at a reference height of 10 m, which is tabulated in both the HEXOS and FASTEX datasets. The solid line at one is the desired result; the dashed line is the best fit through the data. The cloud of points averages 1.1249, and the correlation coefficient is 0.2609.

In (4.3),  $L_v$  is the latent heat of vaporization (Andreas 2005b), and  $r(\tau_f)$  is the droplet radius when the droplet falls back into the sea. Equation (4.3) is in two parts simply to speed the computations: for  $\tau_f > \tau_r$ ,  $r(\tau_f)$  is, in effect,  $r_{eq}$  (Andreas 1992; Andreas and DeCosmo 2002; Andreas et al. 2008).

The first issue in evaluating the total air–sea enthalpy flux, (2.2), is to decide whether spray makes any difference. That is, do we really need to augment the COARE version 2.6 estimates of the interfacial fluxes  $H_s$  and  $H_L$  with spray contributions, as (2.2) implies (cf. Andreas and DeCosmo 2002; Andreas et al. 2008)? Figures 3 and 4 answer this question.

Figure 3 shows the ratio of the measured total enthalpy flux,

$$Q_{en,T} = H_{L,T} + H_{s,T}, \quad (4.5)$$

to the modeled interfacial enthalpy flux,

$$Q_{en,int} = H_L + H_s. \quad (4.6)$$

In these,  $H_{L,T}$  and  $H_{s,T}$  are the HEXOS and FASTEX flux measurements, and  $H_L$  and  $H_s$  are estimates of the interfacial fluxes from the COARE version 2.6 algorithm.

If the COARE algorithm were sufficient for predicting the total enthalpy flux, the ratios  $Q_{en,T}/Q_{en,int}$  in Fig. 3 would not depend on wind speed, and the average of all values would be one. That is, the COARE algorithm

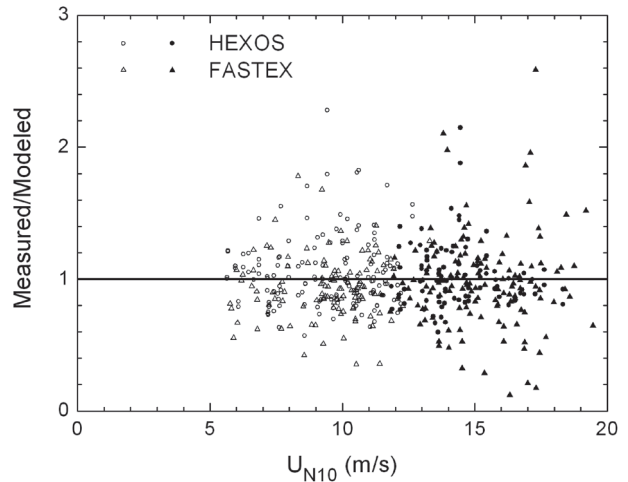


FIG. 4. As in Fig. 3, except here I add spray effects to the interfacial fluxes ( $H_L$  and  $H_s$ ) in (2.2) by setting  $\beta = 18.08$  and  $\gamma = 0$ . The points in the figure now average 0.9991, and the correlation coefficient of the enthalpy flux ratio with  $U_{N10}$  is 0.0000. That is, the best-fit line through the data is indistinguishable from the solid line at one. Filled symbols are cases for which the spray enthalpy flux  $\beta Q_s$  is at least 10% of the interfacial enthalpy flux,  $H_L + H_s$ .

alone would explain both the magnitude and the wind speed dependence of the HEXOS–FASTEX dataset. Figure 3 demonstrates, however, that the COARE version 2.6 algorithm is inadequate on both counts. Using statistics described in Andreas et al. (2008) and the average of the points in Fig. 3, 1.1249, I can reject at the 1% significance level the hypothesis that  $Q_{en,T}/Q_{en,int}$  can be one, on average. Likewise, with the computed correlation coefficient, 0.2609, I can reject at the 1% significance level the hypothesis that  $Q_{en,T}/Q_{en,int}$  is independent of wind speed. In other words, the model, without spray, is biased low and does not explain the wind dependence of the data.

Both of these tests suggest enhanced enthalpy transfer with increasing wind speed. This is a possible signature of spray effects (Andreas and DeCosmo 2002). Hence, the next issue is whether the candidate expression for the total enthalpy flux, (2.2), which combines interfacial and spray contributions, can explain this enhanced transfer. Figure 4 demonstrates that it can.

Figure 4 is like Fig. 3—the ratio of measured-to-modeled enthalpy fluxes. But in Fig. 4, I account for spray effects by adjusting  $\beta$  and  $\gamma$  in (2.2). Actually, I produced Fig. 4 with  $\gamma$  set to zero. That is, I explain the magnitude and the wind speed dependence of the HEXOS and FASTEX enthalpy fluxes by finding just the  $\beta$  value for which the cloud of points in Fig. 4 averages one and the correlation coefficient is essentially zero. With  $\beta = 18.08$  (and  $\gamma = 0$ ), (2.2) meets both

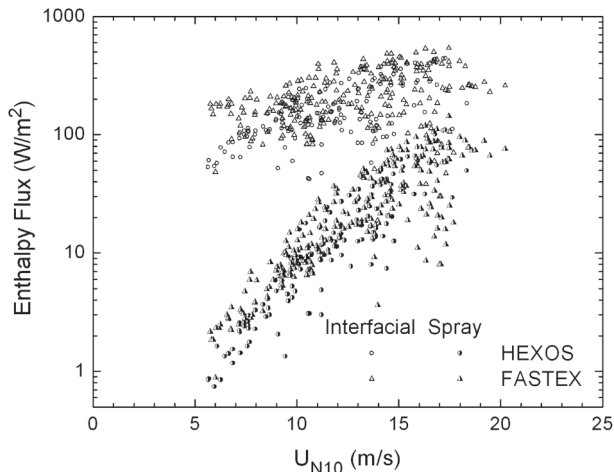


FIG. 5. The modeling described in the text has separated the measured HEXOS and FASTEX total enthalpy fluxes into contribution from the interfacial flux ( $Q_{en,int}$ ) and from the spray-mediated flux ( $Q_{en,sp}$ ). The  $U_{N10}$  is the neutral-stability wind speed at a reference height of 10 m.

conditions. The average of the ratios in Fig. 4 is 0.9991, and the correlation coefficient is 0.0000.

I see no a priori guarantee that the flux algorithm (2.2), with one adjustable spray parameter, must center the cloud of points in Fig. 4 around 1 and simultaneously remove the wind speed dependence in the data. The fact that my simple theoretically based algorithm can do both gives it credence.

The filled symbols in Fig. 4 demonstrate that spray processes begin to have a significant effect on the total air–sea enthalpy flux at modest wind speeds. For these filled symbols, the modeled spray enthalpy flux ( $\beta\bar{Q}_s$ ) is at least 10% of the modeled interfacial enthalpy flux ( $H_L + H_s$ ). Most of the points for  $U_{N10}$  greater than 12 m s<sup>-1</sup> are filled.

In effect, this analysis separates the total measured enthalpy flux into interfacial ( $Q_{en,int}$ ) and spray ( $Q_{en,sp}$ ) contributions:

$$Q_{en,int} = H_L + H_s \quad \text{and} \quad (4.7a)$$

$$Q_{en,sp} = \beta\bar{Q}_s. \quad (4.7b)$$

Here,  $Q_{en,int}$  comes fairly quickly from the COARE algorithm. But finding  $Q_{en,sp}$  involves integrating over the contributions for all spray droplets with radii ( $r_0$ ) between 1.6 and 500  $\mu\text{m}$  and is, therefore, too computationally intensive for any large-scale modeling.

Figure 5 demonstrates this partitioning into interfacial and spray contributions and reiterates the increasing importance of the spray enthalpy flux with increasing wind speed. In Fig. 5, the interfacial enthalpy flux in-

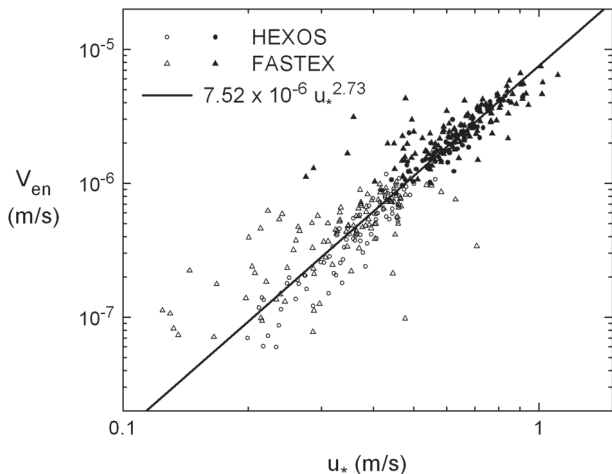


FIG. 6. The wind function  $V_{en}$  in (4.8) as evaluated from the HEXOS and FASTEX enthalpy flux data according to (4.9). The correlation coefficient is 0.917. The line is (4.10), where  $u_*$  is the measured friction velocity. Filled symbols denote cases for which the modeled spray enthalpy flux ( $\beta\bar{Q}_s$ ) is at least 10% of the modeled interfacial enthalpy flux ( $H_L + H_s$ ).

creases modestly with wind speed—approximately linearly. The spray-mediated enthalpy flux, on the other hand, increases as the second or third power of the wind speed and is overtaking the interfacial flux.

We had noticed that droplets with  $r_0$  values near 100  $\mu\text{m}$  dominate the spray sensible heat flux (Andreas and Emanuel 2001; Perrie et al. 2005; Andreas et al. 2008). Hence, as a fast spray enthalpy flux algorithm, I follow Andreas and Emanuel’s (2001) lead and assume that 100- $\mu\text{m}$  droplets are reliable indicators of the spray enthalpy flux. The fast flux parameterization thus becomes [cf. (4.1)]

$$Q_{en,sp} = \beta\bar{Q}_s = \rho_w c_w (T_s - T_{eq,100}) V_{en}(u_*). \quad (4.8)$$

Here,  $T_{eq,100}$  is the equilibrium temperature of droplets that start with radius  $r_0 = 100 \mu\text{m}$ .

Also in (4.8),  $V_{en}(u_*)$  is a wind function: it depends only on the friction velocity  $u_*$  and has units of meters per second. I evaluate it from my partitioning of the HEXOS and FASTEX data as

$$V_{en}(u_*) = \frac{Q_{en,sp}}{\rho_w c_w (T_s - T_{eq,100})}, \quad (4.9)$$

where the  $Q_{en,sp}$  are the spray fluxes shown in Fig. 5. Figure 6 shows the calculations of  $V_{en}(u_*)$ . Here,  $u_*$  is the measured friction velocity, and I evaluated  $T_{eq,100}$  from my fast spray microphysical algorithms (Andreas 2005a).

The data in Fig. 6 cluster well around the power-law relation

$$V_{\text{en}}(u_*) = 7.52 \times 10^{-6} u_*^{2.73}, \quad (4.10)$$

which gives  $V_{\text{en}}$  in meters per second when  $u_*$  is in meters per second. The evidence in Fig. 6 that (4.8) and (4.10) represent the spray enthalpy flux fairly well justifies the validity of such a simple parameterization.

Equation (4.10) gives somewhat smaller values for  $V_{\text{en}}$  than the corresponding relation in Andreas and Emanuel [2001; see their Eq. (8)], which was based on just the HEXOS data. The wind speed dependence in (4.10) (i.e.,  $u_*^{2.73}$ ), however, is almost as strong as Andreas and Emanuel found (i.e.,  $u_*^3$ ) and reiterates why spray processes become increasingly important in storm winds.

The filled symbols in Fig. 6 again denote cases for which the modeled spray enthalpy flux is at least 10% of the corresponding interfacial flux. Most symbols for which  $u_* > 0.5 \text{ m s}^{-1}$  are filled and therefore indicate a significant spray contribution to the total enthalpy flux.

## 5. Spray-mediated salt flux

Equations (4.3) and (4.4) give the nominal spray latent heat flux  $\overline{Q}_L$ . But as I explained earlier, only droplets that experience some evaporation and then fall back into the sea can accomplish a salt flux to the ocean. Equation (4.3a) represents most of these droplets, although there is an uncertain range around  $\tau_f = \tau_r$  for which it is unclear whether a droplet remains suspended or is reentrant. Based on our current understanding, (4.3a) gives the best accounting for droplets that contribute to the spray salt flux.

If the interfacial latent heat flux is  $H_L$ , the associated salt flux is

$$F_{\text{salt}} = \frac{sH_L}{L_v(1-s)}. \quad (5.1)$$

Here,  $s$  is the fractional salinity. That is, if the salinity  $S$  is 34 psu,  $s = 0.034$ . My sign convention is that, if  $H_L$  is positive, the vapor flux is upward—from ocean to atmosphere. Consequently,  $F_{\text{salt}}$  is positive when the salt flux is into the ocean surface. Here,  $F_{\text{salt}}$  has units of kilograms of salt per square meter of sea surface per second.

In analogy with (5.1), I adapt (4.3a) to give the approximate spray salt flux to the ocean that is contributed by droplets of initial radius  $r_0$ :

$$Q_{\text{salt}}(r_0) = \frac{\rho_w s}{1-s} \left\{ 1 - \left[ \frac{r(\tau_f)}{r_0} \right]^3 \right\} \left( \frac{4\pi r_0^3}{3} \frac{dF}{dr_0} \right), \quad (5.2)$$

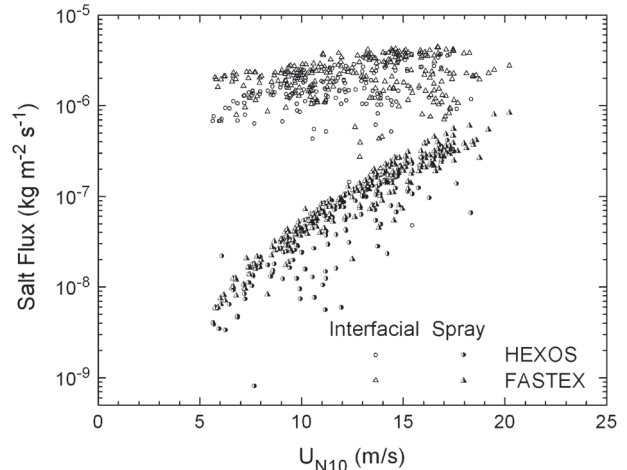


FIG. 7. The interfacial ( $F_{\text{salt}}$ ) and spray ( $Q_{\text{salt,sp}}$ ) salt fluxes are computed from the HEXOS and FASTEX data using (5.1) and (5.4), respectively, and are plotted against the neutral-stability wind speed at a height of 10 m.

for  $\tau_f \leq \tau_r$ . In turn, the nominal spray-mediated salt flux is

$$\overline{Q}_{\text{salt}} = \int_{r_{\text{min}}}^{500} Q_{\text{salt}}(r_0) dr_0, \quad (5.3)$$

where  $r_{\text{min}}$  is the value of  $r_0$  for which  $\tau_f(r_0) = \tau_r(r_0)$  and is a function of wind speed and other environmental conditions.

In tuning the nominal spray latent heat flux  $\overline{Q}_L$  to produce an accurate estimate of the spray latent heat flux  $\alpha \overline{Q}_L$ , Andreas et al. (2008) had the luxury of using data to evaluate  $\alpha$  to be 1.50. Without such data for tuning the spray salt flux, I can only assume that the same tuning coefficient applies to the salt flux. That is, I estimate the spray salt flux as

$$Q_{\text{salt,sp}} = \alpha \overline{Q}_{\text{salt}}, \quad (5.4)$$

where  $\alpha$  is still 1.50.

Figure 7 shows calculations of the interfacial and spray salt fluxes based on the HEXOS and FASTEX data. As earlier,  $H_L$  in (5.1) comes from my adaptation of the COARE version 2.6 algorithm (see Andreas et al. 2008), and  $\overline{Q}_{\text{salt}}$  in (5.4) comes from my full microphysical model. The interfacial salt flux is generally somewhat larger than  $10^{-6} \text{ kg m}^{-2} \text{ s}^{-1}$  and increases slightly as  $U_{\text{N10}}$  increases from 5 to 20  $\text{m s}^{-1}$ . The spray salt flux, in contrast, is less than  $10^{-8} \text{ kg m}^{-2} \text{ s}^{-1}$  in a 5  $\text{m s}^{-1}$  wind but increases dramatically to almost  $10^{-6} \text{ kg m}^{-2} \text{ s}^{-1}$  for a 20  $\text{m s}^{-1}$  wind.

Figure 7 implies that, for wind speeds above the range for which I have data, the spray salt flux will likely

become comparable to or even exceed the interfacial salt flux. Such a flux to the ocean is in no current models but will affect ocean stratification and, thus, ocean mixing in storm winds. Adding a spray salt flux in coupled ocean–atmosphere models may therefore help explain changes in the intensity of tropical cyclones.

Just as the interfacial latent heat flux  $H_L$  is often interpreted in terms of a freshwater or a buoyancy flux at the air–sea interface (e.g., Turner 1979, pp. 130, 163; Gill 1982, pp. 36f, 87f; Kraus and Businger 1994, p. 214),  $Q_{\text{salt,sp}}$  can be converted to a spray-mediated freshwater flux ( $W_{\text{sp}}$ ) and a spray-mediated buoyancy flux ( $B_{\text{sp}}$ ) if an application requires those quantities. Because only re-entrant spray droplets can change the freshwater concentration at the sea surface,

$$W_{\text{sp}} = \left(\frac{1-s}{s}\right)Q_{\text{salt,sp}}, \quad (5.5)$$

which has units of kilograms of water per square meter of sea surface per second. In (5.5),  $Q_{\text{salt,sp}}$  is positive when spray adds salt to the ocean surface. Therefore, positive  $W_{\text{sp}}$  means a loss of freshwater from the ocean.

Realize that  $W_{\text{sp}}$  is always smaller in magnitude than the rate at which vapor is added to the atmosphere by evaporating spray droplets—that is,  $\alpha\bar{Q}_L/L_v$ . This latter quantity includes all the vapor left in the air by evaporating spray and is, thus, a component of the vapor flux measured with eddy-covariance instruments. But because some of the droplets providing this vapor remain suspended indefinitely (i.e., the smaller droplets), their contribution can be viewed as removing a parcel of water from the ocean and holding it suspended in the air. That process may change the total volume of the ocean, but it has not changed the ocean’s temperature or salinity and, thus, has no effect on ocean dynamics. The freshwater flux  $W_{\text{sp}}$ , in contrast, affects ocean dynamics because it changes the surface water density.

Following Gill (1982, p. 37), I also easily obtain the spray-mediated buoyancy flux from  $Q_{\text{salt,sp}}$  as

$$B_{\text{sp}} = g\beta_s Q_{\text{salt,sp}}, \quad (5.6)$$

which has units of  $\text{N m}^{-2} \text{s}^{-1}$ . Here,  $g$  is the acceleration of gravity,  $\beta_s = \rho_s^{-1}\partial\rho_s/\partial s$  is the seawater salinity expansion coefficient, and  $\rho_s$  is the density of seawater. Again,  $B_{\text{sp}}$  is positive when  $Q_{\text{salt,sp}}$  is positive—when re-entrant spray is adding excess salt at the water surface. In turn, a positive buoyancy flux destabilizes the ocean and fosters overturning.

My method for computing (5.4) here is computationally intense. As with the spray enthalpy flux, we need a faster algorithm. When faced with a similar requirement,

Andreas et al. (2008) postulated that spray droplets that start with a radius  $r_0$  of  $50 \mu\text{m}$  are good indicators of the spray latent heat flux. Because  $\tau_f \leq \tau_r$  for these droplets and because the peak in the  $Q_{\text{salt}}(r_0)$  spectrum is near  $50 \mu\text{m}$ , I postulate that  $50\text{-}\mu\text{m}$  droplets are also key indicators of the spray salt flux. My fast flux algorithm thus becomes [cf. (5.2)]

$$Q_{\text{salt,sp}} = \frac{\rho_w s}{1-s} \left\{ 1 - \left[ \frac{r(\tau_{f,50})}{50 \mu\text{m}} \right]^3 \right\} V_{\text{salt}}(u_*), \quad (5.7)$$

where the  $\alpha$  in (5.4) is incorporated into the wind function  $V_{\text{salt}}$ . In (5.7),  $\tau_{f,50}$  is the residence time of droplets that start with a radius of  $50 \mu\text{m}$ ; hence, the  $50 \mu\text{m}$  also takes the place of  $r_0$  in (5.2). Furthermore, I estimate  $r(\tau_{f,50})$  from (2.5) in the form

$$r(\tau_{f,50}) = r_{\text{eq},50} + (50 \mu\text{m} - r_{\text{eq},50}) \exp\left(\frac{-\tau_{f,50}}{\tau_{r,50}}\right), \quad (5.8)$$

where all radii are in micrometers. Andreas’s (2005a) fast microphysical algorithm—rather than the full microphysical model—provides  $r_{\text{eq},50}$  and  $\tau_{r,50}$ , the equilibrium radius of droplets that start at  $50 \mu\text{m}$  and the time scale for that evolution, respectively.

The remaining unknown in (5.7) is  $V_{\text{salt}}(u_*)$ . The spray salt flux data plotted in Fig. 7 provide this as

$$V_{\text{salt}}(u_*) = \frac{Q_{\text{salt,sp}}}{\frac{\rho_w s}{1-s} \left\{ 1 - \left[ \frac{r(\tau_{f,50})}{50 \mu\text{m}} \right]^3 \right\}}. \quad (5.9)$$

Figure 8 shows this function.

The best-fitting line in Fig. 8 is

$$V_{\text{salt}}(u_*) = 8.01 \times 10^{-8} u_*^{2.11}, \quad (5.10)$$

which give  $V_{\text{salt}}$  in meters per second for  $u_*$  in meters per second. The data in Fig. 8 scatter about this line more than the data in Fig. 6 scatter about their fitting line. But the facts that the data cluster around this power-law relation and have a correlation coefficient of 0.765 argue for the usefulness of (5.7) as a good place to start in parameterizing the spray salt flux to the ocean in models.

As with the enthalpy flux in Fig. 6, the filled symbols in Fig. 8 denote cases for which the modeled spray salt flux is at least 10% of the modeled interfacial salt flux. Many symbols for which  $u_* > 0.5 \text{ m s}^{-1}$  are filled.

If an application requires the spray-mediated freshwater ( $W_{\text{sp}}$ ) or buoyancy ( $B_{\text{sp}}$ ) flux rather than  $Q_{\text{salt,sp}}$ , we can simply convert the  $Q_{\text{salt,sp}}$  values computed from (5.7), (5.8), and (5.10) to  $W_{\text{sp}}$  or  $B_{\text{sp}}$  using (5.5) or (5.6), respectively.

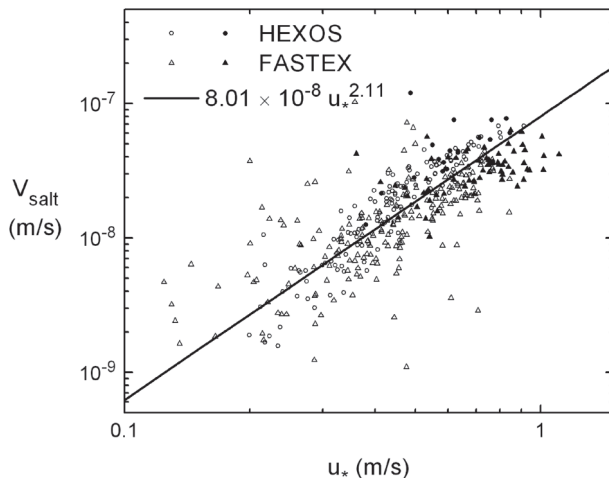


FIG. 8. The wind function  $V_{\text{salt}}$  in (5.7) as evaluated from the HEXOS and FASTEX salt flux data according to (5.9). The correlation coefficient is 0.765. The line is (5.10), where  $u_*$  is the measured friction velocity. Filled symbols denote cases for which the spray salt flux [ $\alpha Q_{\text{salt}}$  from (5.4)] is at least 10% of the interfacial salt flux [ $F_{\text{salt}}$  from (5.1)].

## 6. Discussion

Figures 5 and 7 hint at the tendencies with increasing wind speed of the interfacial and spray enthalpy and salt fluxes. The spray algorithms that I developed in the last two sections give us the tools to extrapolate these fluxes to the lower limits of hurricane-strength winds—to  $40 \text{ m s}^{-1}$ . Such an extrapolation is reasonable because the interfacial flux algorithm is based on the theoretical model of Liu et al. (1979), which was adapted for use in the COARE version 2.6 algorithm (Fairall et al. 1996). Furthermore, the COARE version 2.6 algorithm is well verified in wind speeds up to  $10 \text{ m s}^{-1}$ , where spray-mediated transfer is negligible. In other words, this interfacial transfer theory is well validated.

Likewise, because my spray flux model is based on microphysical theory (e.g., Andreas 1990, 1992, 2005a), because the required spray generation function is constrained by theory (Andreas 2002), and because the resulting flux algorithm is validated for winds up to  $20 \text{ m s}^{-1}$ , I believe it can be reliably extrapolated to  $40 \text{ m s}^{-1}$ . The main issue here is that, for wind speeds between  $30$  and  $40 \text{ m s}^{-1}$ , momentum exchange at the sea surface may undergo a transition. The debate is still open on this issue, but observations in tropical cyclones (Powell et al. 2003), studies in wind-wave tunnels (Donelan et al. 2004), and theoretical models (Kudryavtsev and Makin 2007) suggest that, in the wind speed range  $30$ – $40 \text{ m s}^{-1}$ , the drag coefficient may level off—instead of continuing to increase as predicted by Charnock’s relation.

Such a transition would affect my algorithm’s predictions of both the spray and interfacial fluxes because

the algorithm uses Charnock’s relation to predict the roughness length  $z_0$  (Andreas et al. 2008), which is required for computing  $u_*$  and, in turn,  $H_s$ ,  $H_L$ ,  $Q_{\text{en,sp}}$ , and  $Q_{\text{salt,sp}}$ . As an example of how accurate my algorithm might be when extrapolated to wind speeds between  $30$  and  $40 \text{ m s}^{-1}$ , consider Fig. 2 in Donelan et al. (2004). This figure suggests that the 10-m, neutral-stability drag coefficient  $C_{\text{DN}10}$  begins to level off at a value of about  $2.4 \times 10^{-3}$  once  $U_{\text{N}10}$  reaches  $30 \text{ m s}^{-1}$ . Their drag coefficient at  $30 \text{ m s}^{-1}$ , however, predicts essentially the same friction velocity at this wind speed as the Charnock relation in my algorithm. As a result, my predictions for  $V_{\text{en}}(u_*)$  (and thus  $Q_{\text{en,sp}}$ ) and  $V_{\text{salt}}(u_*)$  (and thus  $Q_{\text{salt,sp}}$ ) at  $U_{\text{N}10} = 30 \text{ m s}^{-1}$  are compatible with observed drag coefficients at  $30 \text{ m s}^{-1}$ .

When  $U_{\text{N}10}$  reaches  $40 \text{ m s}^{-1}$ , the Charnock relation in my algorithm (Charnock constant of 0.0185) predicts that  $u_*$  is  $2.3 \text{ m s}^{-1}$ , while Fig. 2 in Donelan et al. (2004) would imply  $u_* \sim 2.0 \text{ m s}^{-1}$ . Consequently, from (4.10) and (5.10), my algorithm would overestimate  $Q_{\text{en,sp}}$  at  $U_{\text{N}10} = 40 \text{ m s}^{-1}$  by about 46% and  $Q_{\text{salt,sp}}$  by about 34% compared to using the drag coefficient reported by Donelan et al. Remember, though, that the true behavior of the drag coefficient for wind speeds above  $30 \text{ m s}^{-1}$  is still unresolved.

Figure 9 therefore makes predictions of  $Q_{\text{en,int}}$ ,  $Q_{\text{en,sp}}$ ,  $F_{\text{salt}}$ , and  $Q_{\text{salt,sp}}$  up to only  $40 \text{ m s}^{-1}$ , at which wind speed the relevant theories are still approximately accurate. These sample flux predictions are for conditions representative of tropical storms. The two panels present the interfacial and spray components of both the enthalpy flux to the atmosphere and the salt flux to the ocean. Because the spray fluxes depend more strongly on wind speed than do the interfacial fluxes, both spray fluxes are predicted to overtake the corresponding interfacial flux by the time the wind speed reaches  $40 \text{ m s}^{-1}$ . Furthermore, at  $14 \text{ m s}^{-1}$  in the enthalpy plot and at  $18 \text{ m s}^{-1}$  in the salt plot, the spray flux reaches 10% of the interfacial flux and, thus, is making a significant contribution to the total air–sea flux of the constituent.

Through reentrant spray, the spray enthalpy flux cools the ocean, as does the interfacial enthalpy flux. Likewise, reentrant spray constitutes a salt flux at the ocean surface, as does interfacial evaporation. These realizations suggest an alternative approach for measuring the air–sea fluxes that dictate storm intensity: make measurements in the ocean instead of in the atmosphere.

We will likely not improve our ability to predict storm intensity without reliable measurements of the air–sea fluxes in storm winds. Obtaining such measurements, however, is not easy. Traditionally, such data come from fast-responding eddy-covariance instruments mounted on a permanent platform, deployed on a ship or buoy, or

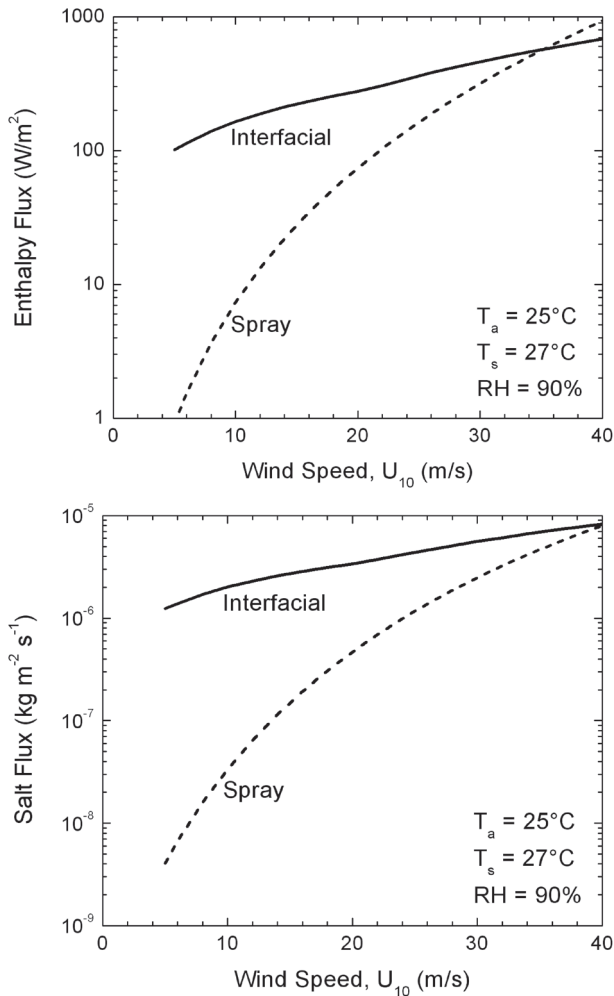


FIG. 9. Algorithm predictions of the interfacial and spray contributions to the enthalpy flux to the atmosphere and the salt flux to the ocean. The interfacial enthalpy flux comes from (4.6); the spray enthalpy flux, from (4.8) and (4.10). The interfacial salt flux comes from (5.1); the spray salt flux, from (5.7), (5.8), and (5.10). Conditions are representative of tropical storms: the sea surface temperature ( $T_s$ ) is  $27^\circ\text{C}$ , the air temperature ( $T_a$ ) is  $25^\circ\text{C}$ , the relative humidity (RH) is 90%, the barometric pressure is 1000 mb, the surface salinity is 34 psu, and the water depth is 3000 m.

fixed to an aircraft. But platforms are often evacuated when cyclone winds are forecast, and ships' captains prefer to avoid cyclones. Moreover, cyclone winds often damage turbulence instruments on platforms, ships, and buoys. Aircraft instruments are usually more robust, but even aircraft flights dedicated to obtaining flux measurements in tropical cyclones are restricted by safety concerns from flying close enough to the sea surface to measure the true surface fluxes. As a result, flight-level fluxes must be extrapolated to the surface, and the uncertainties inherent in those extrapolations are large (e.g., French et al. 2007; Drennan et al. 2007; Zhang et al.

2008). The need to correct for ship and aircraft motion in high winds also increases the uncertainty in atmospheric flux measurements.

Measurements in the oceanic mixed layer could obviate many of these shortcomings in atmospheric flux measurements. For instance, the oceanic instruments will likely survive even hurricane-strength winds; and if the instruments are moored or autonomous and, thus, unattended, no personnel will be put in harm's way. My algorithm suggests that, in high winds, both the temperature and the salinity signals from spray-mediated processes should be observable with current oceanic instruments, although complementary modeling will be necessary to separate those spray components from the interfacial components and from mixing across the thermocline. D'Asaro (2003), Sanford et al. (2007), Jarosz et al. (2007), and Zedler et al. (2009) have reported attempts at such ocean measurements for studying storm processes.

## 7. Conclusions

Tropical cyclones extract enthalpy from the ocean as their source of power. Traditionally, that enthalpy transfer is parameterized as an exchange across the air–sea interface. But theory and observations suggest that that interfacial enthalpy exchange is not large enough to explain storm intensity. Here, I have shown that spray-mediated enthalpy transfer augments the interfacial transfer; this spray enthalpy flux may be a missing piece required for explaining storm intensity.

I have demonstrated the importance of the spray enthalpy flux by using eddy-covariance measurements of the sensible and latent heat fluxes from HEXOS and FASTEX. The sum of these fluxes is the total measured air–sea enthalpy flux. A state-of-the-art flux algorithm that treats just the interfacial transfer cannot, however, reproduce this total enthalpy flux. Only when I add a theoretically based model for the spray-mediated enthalpy flux to the interfacial flux algorithm can I explain both the magnitude and the wind speed dependence of the HEXOS and FASTEX data.

These calculations essentially separated the HEXOS and FASTEX flux measurements into interfacial and spray enthalpy fluxes. From the spray fluxes, I then developed a fast algorithm for predicting the spray enthalpy flux in large-scale models. That algorithm is based on the premise that droplets with an initial radius of  $100\ \mu\text{m}$  are bellwethers of the spray enthalpy flux and introduces a wind function  $V_{\text{en}}$  that goes as  $u_*^{2.73}$ , where  $u_*$  is the friction velocity. This strong dependence on  $u_*$  emphasizes why spray processes are important in storm winds.

Building on Andreas and Emanuel's (2001) idea of reentrant spray, I realized that spray droplets constitute an effective salt flux to the ocean when they reenter it. Again using my full spray microphysical model and the HEXOS and FASTEX data, I made the first estimate of this spray salt flux. It starts lower but increases more rapidly with wind speed than the salt flux resulting from interfacial evaporation and likely will dominate the salt flux to the ocean in hurricane-force winds.

From the spray salt flux that my modeling deduced from the HEXOS and FASTEX data, I developed a fast algorithm for estimating the spray salt flux for use in large-scale models. This algorithm presumes that droplets that start with radii of 50  $\mu\text{m}$  are good indicators of the spray salt flux. The wind function  $V_{\text{salt}}$ , which is key to this algorithm, goes as  $u_*^{2.11}$ . Thus, as with enthalpy, the spray salt flux becomes increasingly important in storm winds.

The spray salt flux is directly related to the spray-mediated freshwater and buoyancy fluxes at the sea surface. My algorithm also predicts these two quantities.

Because I find that, in storm winds, spray-mediated enthalpy and salt fluxes produce signals in the ocean that are comparable in magnitude to the signals from the interfacial enthalpy and salt fluxes, I raise the possibility of measuring the air-sea fluxes relevant to predicting storm intensity with instruments in the ocean rather than in the atmosphere. The main advantage of such oceanic measurements is that the instruments will survive hurricane-strength winds.

Andreas et al. (2008) added to the COARE version 2.6 bulk interfacial flux algorithm an algorithm that makes fast calculations of the spray-mediated fluxes of momentum and sensible and latent heat. They made their FORTRAN code publicly available. I have now added calculations of the interfacial and spray enthalpy and salt fluxes to that algorithm and offer this code to anyone interested in running it.

*Acknowledgments.* I thank Ola Persson, Jeff Hare, Chris Fairall, and Bill Otto for providing the FASTEX data and Emily Andreas Moynihan for help with the graphics. Two anonymous reviewers offered useful comments that helped me improve the manuscript. The Office of Naval Research supported this work with Grant N000140810411.

#### REFERENCES

- Andreas, E. L., 1989: Thermal and size evolution of sea spray droplets. CRREL Rep. 89-11, U.S. Army Cold Regions Research and Engineering Laboratory, Hanover, NH, 37 pp. [NTIS ADA210484.]
- , 1990: Time constants for the evolution of sea spray droplets. *Tellus*, **42B**, 481–497.
- , 1992: Sea spray and the turbulent air-sea heat fluxes. *J. Geophys. Res.*, **97**, 11 429–11 441.
- , 1995: The temperature of evaporating sea spray droplets. *J. Atmos. Sci.*, **52**, 852–862.
- , 1996: Reply. *J. Atmos. Sci.*, **53**, 1642–1645.
- , 2002: A review of the sea spray generation function for the open ocean. *Atmosphere-Ocean Interactions*, Vol. 1, W. Perrie, Ed., WIT Press, 1–46.
- , 2005a: Approximation formulas for the microphysical properties of saline droplets. *Atmos. Res.*, **75**, 323–345.
- , 2005b: *Handbook of Physical Constants and Functions for Use in Atmospheric Boundary Layer Studies*. ERDC/CRREL Monogr. No. M-05-1, U.S. Army Cold Regions Research and Engineering Laboratory, 42 pp.
- , and J. DeCosmo, 1999: Sea spray production and influence on air-sea heat and moisture fluxes over the open ocean. *Air-Sea Exchange: Physics, Chemistry and Dynamics*, G. L. Geernaert, Ed., Kluwer, 327–362.
- , and K. A. Emanuel, 2001: Effects of sea spray on tropical cyclone intensity. *J. Atmos. Sci.*, **58**, 3741–3751.
- , and J. DeCosmo, 2002: The signature of sea spray in the HEXOS turbulent heat flux data. *Bound.-Layer Meteor.*, **103**, 303–333.
- , and S. Wang, 2007: Predicting significant wave height off the northeast coast of the United States. *Ocean Eng.*, **34**, 1328–1335.
- , J. B. Edson, E. C. Monahan, M. P. Rouault, and S. D. Smith, 1995: The spray contribution to net evaporation from the sea: A review of recent progress. *Bound.-Layer Meteor.*, **72**, 3–52.
- , P. O. G. Persson, and J. E. Hare, 2008: A bulk turbulent air-sea flux algorithm for high-wind, spray conditions. *J. Phys. Oceanogr.*, **38**, 1581–1596.
- Businger, J. A., 1982: The fluxes of specific enthalpy, sensible heat and latent heat near the earth's surface. *J. Atmos. Sci.*, **39**, 1889–1892.
- Chang, H.-R., and R. L. Grossman, 1999: Evaluation of bulk surface flux algorithms for light wind conditions using data from the Coupled Ocean-Atmosphere Response Experiment (COARE). *Quart. J. Roy. Meteor. Soc.*, **125**, 1551–1588.
- D'Asaro, E. A., 2003: The ocean boundary layer below Hurricane Dennis. *J. Phys. Oceanogr.*, **33**, 561–579.
- DeCosmo, J., 1991: Air-sea exchange of momentum, heat and water vapor over whitecap sea states. Ph.D. dissertation, University of Washington, 212 pp.
- , K. B. Katsaros, S. D. Smith, R. J. Anderson, W. A. Oost, K. Bumke, and H. Chadwick, 1996: Air-sea exchange of water vapor and sensible heat: The Humidity Exchange over the Sea (HEXOS) results. *J. Geophys. Res.*, **101**, 12 001–12 016.
- Donelan, M. A., B. K. Haus, N. Reul, W. J. Plant, M. Stiassnie, H. C. Graber, O. B. Brown, and E. S. Saltzman, 2004: On the limiting aerodynamic roughness of the ocean in very strong winds. *Geophys. Res. Lett.*, **31**, L18306, doi:10.1029/2004GL019460.
- Drennan, W. M., J. A. Zhang, J. R. French, C. McCormick, and P. G. Black, 2007: Turbulent fluxes in the hurricane boundary layer. Part II: Latent heat flux. *J. Atmos. Sci.*, **64**, 1103–1115.
- Emanuel, K. A., 1995: Sensitivity of tropical cyclones to surface exchange coefficients and a revised steady-state model incorporating eye dynamics. *J. Atmos. Sci.*, **52**, 3969–3976.
- Fairall, C. W., J. D. Kepert, and G. J. Holland, 1994: The effect of sea spray on surface energy transports over the ocean. *Global Atmos. Ocean Syst.*, **2**, 121–142.
- , E. F. Bradley, D. P. Rogers, J. B. Edson, and G. S. Young, 1996: Bulk parameterization of air-sea fluxes for Tropical

- Ocean-Global Atmosphere Coupled-Ocean-Atmosphere Response Experiment. *J. Geophys. Res.*, **101**, 3747–3764.
- , —, J. E. Hare, A. A. Grachev, and J. B. Edson, 2003: Bulk parameterization of air–sea fluxes: Updates and verification for the COARE algorithm. *J. Climate*, **16**, 571–591.
- French, J. R., W. M. Drennan, J. A. Zhang, and P. G. Black, 2007: Turbulent fluxes in the hurricane boundary layer. Part I: Momentum flux. *J. Atmos. Sci.*, **64**, 1089–1102.
- Gill, A. E., 1982: *Atmosphere–Ocean Dynamics*. Academic Press, 662 pp.
- Grant, A. L. M., and P. Hignett, 1998: Aircraft observations of the surface energy balance in TOGA-COARE. *Quart. J. Roy. Meteor. Soc.*, **124**, 101–122.
- Jarosch, E., D. A. Mitchell, D. W. Wang, and W. J. Teague, 2007: Bottom-up determination of air–sea momentum exchange under a major tropical cyclone. *Science*, **315**, 1707–1709.
- Joly, A., and Coauthors, 1997: The Fronts and Atlantic Storm-Track Experiment (FASTEX): Scientific objectives and experimental design. *Bull. Amer. Meteor. Soc.*, **78**, 1917–1940.
- Katsaros, K. B., and Coauthors, 1994: Measurements of humidity and temperature in the marine environment during the HEXOS main experiment. *J. Atmos. Oceanic Technol.*, **11**, 964–981.
- Kraus, E. B., and J. A. Businger, 1994: *Atmosphere–Ocean Interaction*. 2nd ed. Oxford University Press, 362 pp.
- Kudryavtsev, V. N., and V. K. Makin, 2007: Aerodynamic roughness of the sea surface at high winds. *Bound.-Layer Meteor.*, **125**, 289–303.
- Liu, W. T., K. B. Katsaros, and J. A. Businger, 1979: Bulk parameterization of air–sea exchanges of heat and water vapor including the molecular constraints at the interface. *J. Atmos. Sci.*, **36**, 1722–1735.
- Perrie, W., L. Andreas, W. Zhang, W. Li, J. Gyakum, and R. McTaggart-Cowan, 2005: Sea spray impacts on intensifying midlatitude cyclones. *J. Atmos. Sci.*, **62**, 1867–1883.
- Persson, P. O. G., J. E. Hare, C. W. Fairall, and W. D. Otto, 2005: Air–sea interaction processes in warm and cold sectors of extratropical cyclonic storms observed during FASTEX. *Quart. J. Roy. Meteor. Soc.*, **131**, 877–912.
- Powell, M. D., P. J. Vickery, and T. A. Reinhold, 2003: Reduced drag coefficient for high wind speeds in tropical cyclones. *Nature*, **422**, 279–283.
- Sanford, T. B., J. F. Price, J. B. Girton, and D. C. Webb, 2007: Highly resolved observations and simulations of the ocean response to a hurricane. *Geophys. Res. Lett.*, **34**, L13604, doi:10.1029/2007GL029679.
- Smith, S. D., and Coauthors, 1992: Sea surface wind stress and drag coefficients: The HEXOS results. *Bound.-Layer Meteor.*, **60**, 109–142.
- Turner, J. S., 1979: *Buoyancy Effects in Fluids*. Cambridge University Press, 368 pp.
- Zedler, S. E., P. P. Niiler, D. Stammer, E. Terrill, and J. Morzel, 2009: Ocean’s response to Hurricane Frances and its implications for drag coefficient parameterization at high wind speeds. *J. Geophys. Res.*, **114**, C04016, doi:10.1029/2008JC005205.
- Zhang, J. A., P. G. Black, J. R. French, and W. M. Drennan, 2008: First direct measurements of enthalpy flux in the hurricane boundary layer: The CBLAST results. *Geophys. Res. Lett.*, **35**, L14813, doi:10.1029/2008GL034374.